

## Non-pathogenic microbiota accelerate age-related CpG Island methylation in colonic mucosa

Ang Sun, Pyounghwa Park, Lauren Cole, Himani Vaidya, Shinji Maegawa, Kelsey Keith, Gennaro Calendo, Jozef Madzo, Jaroslav Jelinek, Christian Jobin & Jean-Pierre J. Issa

To cite this article: Ang Sun, Pyounghwa Park, Lauren Cole, Himani Vaidya, Shinji Maegawa, Kelsey Keith, Gennaro Calendo, Jozef Madzo, Jaroslav Jelinek, Christian Jobin & Jean-Pierre J. Issa (2023) Non-pathogenic microbiota accelerate age-related CpG Island methylation in colonic mucosa, *Epigenetics*, 18:1, 2160568, DOI: [10.1080/15592294.2022.2160568](https://doi.org/10.1080/15592294.2022.2160568)

To link to this article: <https://doi.org/10.1080/15592294.2022.2160568>



© 2023 The Author(s). Published by Informa UK Limited, trading as Taylor & Francis Group.



[View supplementary material](#)



Published online: 26 Dec 2022.



[Submit your article to this journal](#)



Article views: 1642



[View related articles](#)



[View Crossmark data](#)

RESEARCH PAPER



## Non-pathogenic microbiota accelerate age-related CpG Island methylation in colonic mucosa

Ang Sun <sup>a</sup>, Pyounghwa Park <sup>a,b</sup>, Lauren Cole<sup>a</sup>, Himani Vaidya <sup>a,b</sup>, Shinji Maegawa <sup>a,c</sup>, Kelsey Keith <sup>a,b</sup>, Gennaro Calendo <sup>b</sup>, Jozef Madzo <sup>a,b</sup>, Jaroslav Jelinek <sup>a,b</sup>, Christian Jobin <sup>d</sup>, and Jean-Pierre J. Issa <sup>a,b</sup>

<sup>a</sup>Fels Cancer Institute for Personalized Medicine, Temple University School of Medicine, Philadelphia, PA, United States; <sup>b</sup>Coriell Institute for Medical Research, Camden, NJ, United States; <sup>c</sup>Research Department of Pediatrics, University of Texas, MD Anderson Cancer Center Department of Pediatrics, University of Texas, MD Anderson Cancer Center Houston, TX, USA; <sup>d</sup>Department of Medicine, Division of Gastroenterology, Hepatology, and Nutrition, University of Florida College of Medicine, Gainesville, Florida, USA

### ABSTRACT

DNA methylation is an epigenetic process altered in cancer and ageing. Age-related methylation drift can be used to estimate lifespan and can be influenced by extrinsic factors such as diet. Here, we report that non-pathogenic microbiota accelerate age-related methylation drift in the colon when compared with germ-free mice. DNA methylation analyses showed that microbiota and IL10KO were associated with changes in 5% and 4.1% of CpG sites, while mice with both factors had 18% alterations. Microbiota, IL10KO, and their combination altered 0.4%, 0.4%, and 4% of CpG island methylation, respectively. These are comparable to what is seen in colon cancer. Ageing changes were accelerated in the IL10KO mice with microbiota, and the affected genes were more likely to be altered in colon cancer. Thus, the microbiota affect DNA methylation of the colon in patterns reminiscent of what is observed in ageing and colorectal cancer.

### ARTICLE HISTORY

Received 2 May 2022  
Revised 10 October 2022  
Accepted 11 November 2022

### KEYWORDS

DNA methylation;  
Microbiota; Germ-free;  
Inflammation; Ageing

## Introduction


DNA methylation is an epigenetic mark with a profound impact on gene regulation and expression. This mark consists of the addition of a methyl group to a cytosine residue of a CG dinucleotide [1,2]. Approximately 80% of CpG sites in the human genome are methylated [3]. Many CpG sites are located in CpG islands (CGIs); these islands are 500–2000 bp stretches of DNA heavily enriched for C or G bases. They are generally unmethylated and are primarily located around transcription start sites (TSS). Methylation of TSS CGIs leads to gene silencing, but intergenic or gene body methylation can have varying effects, depending on the gene and the exact site that is methylated [4]. Disruption of DNA methylation patterns is associated with ageing and disease; this is characterized by global hypomethylation and aberrant hypermethylation of CGIs [1]. CGI hypermethylation leads to the down-regulation of key genes, including tumour suppressor genes, which can directly result in

tumorigenesis [5,6]. Consequently, studying the causes of aberrant methylation is essential to our understanding of both ageing and cancer. Cell intrinsic factors such as the density of repetitive elements, baseline gene expression, and binding by PCG proteins can affect the propensity to aberrant DNA methylation in cancer [5, 7–10]. Cell extrinsic factors that modulate DNA methylation are less well defined, but they include ageing, diet, and chronic inflammation [1, 11–14].

The human gut microbiota is composed of approximately  $10^{13}$  bacteria, which practically match the number of human cells in the body [15]. The gut microbiota has co-evolved with the host, forming a symbiotic relationship contributing to energy and nutrient extraction from diets, shaping immune response, maintaining intestinal mucosal barrier integrity, and performing key xenobiotic metabolism [16–20]. The gut microbiome is linked to inflammatory diseases, a major risk factor for cancer. In

**CONTACT** Pyounghwa Park  [peaceppark@temple.edu](mailto:peaceppark@temple.edu)  Fels Cancer Institute for Personalized Medicine, Temple University Lewis Katz School of Medicine, Philadelphia, PA, United States; Jean-Pierre J. Issa  [jpissa@coriell.org](mailto:jpissa@coriell.org)  Coriell Institute for Medical Research, 403 Haddon Avenues, Camden, NJ 08103

This article has been republished with minor changes. These changes do not impact the academic content of the article.

 Supplemental data for this article can be accessed online at <https://doi.org/10.1080/15592294.2022.2160568>

© 2023 The Author(s). Published by Informa UK Limited, trading as Taylor & Francis Group.

This is an Open Access article distributed under the terms of the Creative Commons Attribution License (<http://creativecommons.org/licenses/by/4.0/>), which permits unrestricted use, distribution, and reproduction in any medium, provided the original work is properly cited.

addition, the microbiome has been implicated in both ageing and inflammation. Germ-free (GF) mice raised and maintained without a microbiota have extended lifespans relative to their normal counterparts [21]. The microbiota has the ability to induce inflammation [22] and, in turn, inflammation has been shown to significantly alter microbiota composition [23].

Because of the common link to inflammation, there has been an interest in studying potential microbiota/epigenetic interactions. Microbiota have been shown to induce large-scale, diet-dependent changes in histone modifications [24]. A study of eight pregnant women examined the microbial composition and DNA methylation in the gut, finding that CGI methylation profiles differed based on microbial composition [25]. Additionally, infections have been linked to DNA methylation changes in cancer: Infection with *H. pylori* led to methylation of CGI promoters including TSGs in gastric cancer [26]. Also, in gastric cancer, a hypermethylation phenotype termed CpG Island Methylator Phenotype (CIMP) has been linked to Epstein–Barr virus (EBV) presence [27]. It was also shown that a specific family of bacteria, *Fusobacteria*, is markedly enriched in colorectal cancers (CRCs) with CIMP, but much less so in cancers without CIMP [28]. Based on these data, we hypothesized that the microbiota could induce changes in DNA methylation. To test this hypothesis directly, we compared DNA methylation in the colon of wild-type (WT) GF mice and WT mice inoculated with microbiota that were specific-pathogen-free (SPF). Further, we investigated the difference between the colonic DNA methylation of GF and SPF mice in a different genetic background, Interleukin 10 knockout (IL10KO), because IL10 is an anti-inflammatory cytokine and a previous study showed mice lacking the *IL10* gene (*IL10*<sup>-/-</sup>, IL10KO) develop spontaneous intestinal inflammation in the presence of microbiota [29]. We also studied interactions between the presence of microbiota and the DNA methylation of IL10 KO (*IL10*<sup>-/-</sup>) mice (prone to inflammation and tumorigenesis), ageing mice, and mice exposed to the carcinogen azoxymethane (AOM).

## Materials and methods

### Mouse colon samples

Mouse colon tissues for microbiota, IL10KO, and AOM studies were obtained from previously

described experiments testing the effects of microbiota on colonic tumours [23]. IL10KO and WT SPF mice (129/SvEv) were born and raised in germ-free isolators and transferred to SPF facility at ages 7–12 weeks to acquire microbiota from the SPF environment for 20 weeks until sacrificed. Both the GF and SPF mice were born and raised in house at the Center for Gastrointestinal Biology and Disease Gnotobiotic Core animal facility at the University of North Carolina at Chapel Hill. Proximal colon tissues were obtained from the GF and SPF mice, which were sacrificed at approximately 8 months of age via CO<sub>2</sub> inhalation followed by cervical dislocation to ensure death (mice not anaesthetised prior to CO<sub>2</sub> exposure). Mouse colon tissues for ageing studies were obtained from six C57/B6 WT mice kept on regular diets and sacrificed at 4 (n = 3) or 30–33 (n = 3) months of age. Power analysis was performed for the ageing mouse model by calculating average of power for each CpG site with larger than 5% of methylation difference. The average power of the ageing mouse model is 0.90, and insured three mice is sufficient to detect the methylation variability between designed groups. All animal protocols were reviewed and approved by the Institutional Animal Care and Use Committee of the University of North Carolina at Chapel Hill and the Institutional Animal Care and Use Committee of Temple University.

We studied a total of 48 mice (Table 1).

### Digital restriction enzyme analysis of methylation

Digital Restriction Enzyme Analysis of Methylation (DREAM) is a quantitative, deep-sequencing-based method of measuring DNA methylation at CpG sites within the CCCGGG sequence [30,31]. Genomic DNA (gDNA) was extracted from mouse proximal colon tissues as previously described [32]. Then, the gDNA was subjected to constructing libraries for next-generation sequencing following the protocol of performing DREAM published previously [30,31]. Briefly, mouse proximal colonic gDNA was sequentially treated with two restriction enzymes *Sma*I and *Xma*I, which act on the same DNA sequence but leave different 5' ends of fragments. *Sma*I is blocked by CpG methylation, but *Xma*I is not. By treating

**Table 1.** Type and number of mice studied for DNA methylation.

Mouse Model*	Number of Mice	Age at Collection (months)	Comment
WT/GF	6	8	Germ-free (GF) mice – no microbiota
WT/SPF	6	8	Mice with a Specific-Pathogen-Free (SPF) microbiota
IL10KO/GF	6	8	<i>Il10</i> <sup>-/-</sup> are predisposed to spontaneous inflammation but only in the presence of microbiota
IL10KO/SPF	6	8	Azoxymethane (AOM) is a colon carcinogen
WT/SPF + AOM	6	8	Predisposed to spontaneous inflammation and tumorigenesis but only in the presence of microbiota
IL10KO/GF + AOM	6	8	
IL10KO/SPF + AOM	6	8	
Young (C57/B6)	3	4	4 months old
Old (C57/B6)	3	30–33	30–33 months old

\*All mice were 129/SvEv unless noted otherwise.

gDNA first with *Sma*I, then *Xma*I, we create distinct signatures for unmethylated and methylated CpG sites at the edges of restriction fragments. Next, Illumina sequencing adapters were ligated to the ends of the restriction fragments to construct libraries, which were then sequenced by Illumina HiSeq 2500 instrument at the Fox Chase Cancer Center Genomics facility. We aligned the sequencing reads to the mouse genome (mm9) using Bowtie2, and counted signatures corresponding to unmethylated and methylated CpGs. There are 173,451 CCCGGG sites in mm9 genome assembly with 19,673 of them in CpG islands. At a minimum of 100 reads per CpG site, using DREAM, we could detect the methylation status of approximately 25,000 CpG sites on average. The sequencing results were filtered by a minimum sequencing depth of 100 reads on autosomes in at least 75% of the samples. We calculated methylation levels as the ratio of reads with the methylated signature to all reads mapping to each respective sites. The methylation values were then adjusted based on nine spiked-in standards, which have known methylation levels. At each *Sma*I/*Xma*I site, the *Xma* stood for the number of reads corresponding to methylated CpG (i.e., reads starting with CCCGGG), and *Sma* was used as the number of reads corresponding to unmethylated CpG (i.e., reads starting with GGG). Then, the methylation value was calculated as  $100\% \times (c \times (Xma + 0.5) / (c \times (Xma + 0.5) + Sma + 0.5))$ , where *c* was the correction factor calculated based on the observed and expected methylation of spiked-in standards. The correction factor characterizes the efficiency of enzyme digestion. We accepted data with correction factor values between 0.5 and 2.0 (1.0 means no correction).

### Bisulphite pyrosequencing for DNA methylation analysis

Bisulphite treatment of gDNA was performed by using the EpiTect Bisulphite Kit (Qiagen) following the manufacturer's instructions. A quantitative bisulphite pyrosequencing method for DNA methylation analyses was used as previously reported [32–34]. Briefly, bisulphite-treated gDNA was amplified with gene-specific primers in a two-step PCR (Polymerase Chain Reaction). The reverse strand of DNA was labelled with biotin in the second step of the PCR. DNA methylation was quantified and indicated as the percentage of bisulphite-resistant cytosines at CpG sites by pyrosequencing performed following the instructions of the manufacturer using the PyroMark Gold Q96 CDT Reagents (Qiagen) on the PyroMark Q96 MD platform (Qiagen) and analysed by Pyro Q-CpG Software (Qiagen). For each biological sample, an average of three technical replicates were reported. The PCR primer sequences and conditions for bisulphite pyrosequencing of CpG sites in the promoter CGI of *Trhde*, a previously reported ageing-related gene [32], are listed in Supplementary Table 1.

### Quantitative RT-PCR analysis for gene expression

From the mouse proximal colon tissue samples, high-quality total RNA was extracted by using TRIzol (Invitrogen) following the manufacturer's instructions. Then, complementary DNA was prepared by using a High Capacity cDNA Reverse Transcription Kit (Applied Biosystems) and followed the instructions from the manufacturer

and used the total RNA as the template. The expression of *Trhde*, *Srrm4*, and *GAPDH* was quantified by a quantitative real-time polymerase chain reaction (qRT-PCR) performed by a StepOne Real-Time PCR system (Applied Biosystems) using TaqMan gene expression assays (Applied Biosystems).

### Pathway analysis

Pathway analysis was done using the R package ReactomePA, which is an R interface for pathway analysis using the open-source and manually curated Reactome pathway database (<https://reactome.org/>) [35]. Promoters were defined as the transcription start site, plus or minus 1500 bases. Promoters were considered changed if they had at least one significant differential methylation CpG site within them. For background, all promoters with at least one measured CpG were used. P-values were corrected for multiple testing using FDR.

### Multivariate linear regression model for the relationship between methylation and microbiota, IL10KO, and AOM treatment

For each CpG site, we generated a multivariate linear regression for the relationship between methylation and microbiota, IL-10 deficiency, and AOM treatment. The linear equation is defined by Equation [1]  $y = b_m x_m + b_i x_i + b_a x_a + b_0 + \epsilon$ , where  $y$  is methylation,  $x$  is the respective condition ( $m =$  microbiota,  $i =$  IL10KO, or  $a =$  azoxymethane respectively),  $b$  is the respective regression coefficient, and  $\epsilon$  is the error term in predicting the value of  $Y$ .

### Statistical analyses

Statistical analyses were performed, and the figures were generated using R [36] (<https://www.R-project.org/>). Volcano plots were generated by plotting the average difference in methylation for a given CpG site against the negative log<sub>10</sub> of the p-value. Average methylation change was calculated by subtracting average methylation in one condition from another, and an unpaired t-test

was used to calculate a 2-tailed p-value. Bar plots were generated by taking the number of sites meeting a condition dividing by the number of sites examined. UpSet plots were generated using the ggupset package [37], while all other plots were generated using the ggplot2 package. All reported p-values are two-sided, and  $p \leq 0.05$  was used as a threshold of significance.

## Results

### Microbiota modulate DNA methylation

We used DREAM to examine how the presence of microbiota affects DNA methylation. To do this, DREAM data for WT GF and WT SPF mice were analysed and a volcano plot depicting the methylation differences between them was generated (Figure 1a). For most experiments, each group of mice consisted of six animals (Table 1). DREAM detected the methylation status of 24,865 sites on average at a minimum of 100 reads/site. We considered sites to be ‘changed’ if there was a statistically significant increase or decrease in average methylation of 5% or more. To ensure precision, we only analysed autosomal CpG sites that had greater than 100 reads in at least 75% of the mice in each group. Overall, of 12,919 detectable sites, 3.7% decreased, and 1.3% of sites increased in methylation. Thus, 5% of CpG sites analysed showed differences triggered by the presence of microbiota.

CpG sites that are greater than 80% or less than 20% methylated at baseline tend to be more stable than intermediately methylated sites [3]. Therefore, we examined how the microbiota affect different CpG compartments. Volcano plots were generated that looked only at sites with greater than 80% average methylation, sites with less than 20% methylation, and sites with between 20% and 80% methylation in GF mice (Supplementary Figure S1). Overall, 0.3% of unmethylated sites were affected by microbiota, compared to 1.1% of highly methylated sites, and 3.8% of intermediately methylated sites. Figure 1d shows the distribution of sites that were changed at least 5% between GF and SPF mice, stratified by baseline methylation. CpG island (CGI) and CGI shore sites appear to be largely stable. The most vulnerable sites seem to be gene body or intergenic

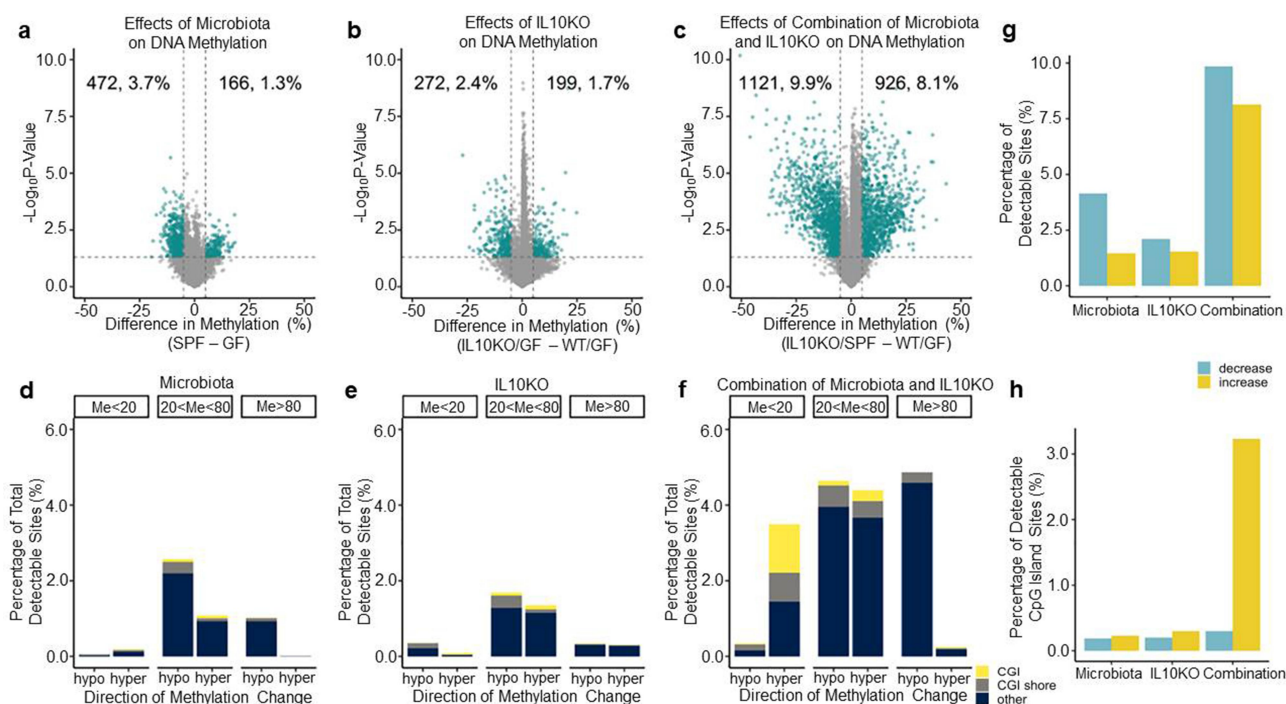


**Figure 1.** Microbiota influence DNA methylation. a-c) Volcano plot analysis showing methylation differences between SPF and GF mice (a), *Il10*<sup>-/-</sup> and GF mice (b), and SPF-*Il10*<sup>-/-</sup> and GF mice (c). The x-axis shows the difference in average methylation between SPF and GF mice for a given site. The y-axis is the negative log(10) of the p-value, which was determined with a Student's t-test. All sites above the dotted line are significant at  $p \leq 0.05$ . Green sites change at a magnitude of 5% or greater. d-f) Bar graphs showing the proportion and type of CpG sites that change at least 5% between SPF and GF mice (d), *Il10*<sup>-/-</sup> and GF mice (e), and SPF-*Il10*<sup>-/-</sup> and GF mice (f). Shore indicates sites that are not in CGIs but within 2,000 bp of them. (g) Bar graph showing the proportion of CpG sites that show DNA methylation alterations in the volcano plots in a-c. (h) Bar graph showing the proportion of CpG sites within CpG islands that show DNA methylation alterations in the volcano plots in a-c.

areas with baseline methylation of between 20% and 80%. Thus, the presence of microbiota significantly affects DNA methylation in colonic mucosa with slightly more pronounced hypomethylation than hypermethylation.

### Deletion of *Il10* affects DNA methylation

*IL10* is an anti-inflammatory cytokine and mice lacking the gene develop spontaneous intestinal inflammation in the presence of microbiota [29]. To determine the effects of *Il10* on colonic DNA methylation independent of microbiota, DREAM data from GF/WT and GF/*IL10*KO mice were compared; Figure 1b shows the volcano plot. Of all detectable sites, 2.4% decreased and 1.7% increased in methylation. Figure 1e shows the distribution of affected sites located in CGIs, CGI shores, or other sites; Like Figure 1d, Figure 1e shows that relatively

fewer CGI/shore sites were subject to change, and most of the changes that did occur were at variable sites with 20% to 80% methylation (also see Supplementary Figure S1). GF/*IL10*KO mice have little detectable inflammation [23]; thus, the DNA methylation changes seen in these animals may be direct effects of *Il10* deficiency or may be related to low grade/patchy inflammation that is not detectable using the usual assays.

*Il10* deficiency combined with microbiota results in inflammation and markedly accelerates colon tumorigenesis in mice [23,38]. By comparing DREAM data from GF/WT to SPF/*IL10*KO mice, we were able to examine the effects from the combination of *IL10* deficiency and the presence of microbiota. In a differential methylation analysis (Figure 1c), we found that 8.1% of sites increased and 9.9% of sites decreased in average methylation. In addition to more sites changing average methylation, the combined effects of inflammation susceptibility and microbiota

appear to be associated with a specific increase in methylation at CGIs and CGI shores. **Figure 1f** shows that 2% of all sites were CGI/CGI shore sites that increased in average methylation between WT/GF and IL10KO/SPF mice. This contrasted with the individual effects from IL10 deficiency or microbiota, which had little impact on CGIs or CGI shores. **Figure 1g** gives a broad overview of the effects of microbiota and IL10KO on DNA methylation individually and together. Both microbiota and IL10KO changed methylation at approximately 4–5% of sites. When combined, approximately 18% of sites experienced average methylation changes, with more sites decreasing in average methylation than increasing. When we examined CGIs exclusively (**Figure 1h**), 0.4% were changed by microbiota, 0.5% were changed by IL10KO while 3.5% were changed by the combination of microbiota and IL10-deficiency. These dramatic differences in DNA methylation are comparable to what can be seen when comparing cancer to normal [34].

### **Differential effects of AOM and IL10KO on DNA methylation**

AOM is a carcinogen commonly used to induce colorectal tumorigenesis in mouse models. We sought to determine if AOM and IL10KO differed in their effects on DNA methylation profiles. We examined the effects of AOM alone, IL10KO alone, and both in combination in the presence of microbiota (i.e., in SPF mice). A differential methylation analysis showed that AOM had a pronounced hypomethylating effect (**Figure 2a**). As a result of AOM treatment, approximately 8.1% of sites decreased in average methylation, as opposed to only 1.2% of sites increasing in average methylation. It is interesting to note that in both sites with 80% or more average methylation and 20% or less average methylation, AOM affected overall decreases in average methylation (**Figure 2b**). In addition, AOM did not seem to target CGI or CGI shore sites and was most likely associated with a decrease in methylation of sites with medium levels of baseline methylation (20% < Me < 80%, **Figure 2b**). By contrast, IL10KO in SPF mice led to 5.7% of sites decreasing in methylation and 6.2% of sites increasing in methylation (**Figure 2c**); about one-third of sites that increased

in methylation were located in CGIs or CGI shores (**Figure 2d**). Thus, AOM and IL10KO both induced hypomethylation but, in the presence of microbiota, only IL10KO induced substantial CGI hypermethylation, pointing to potentially different mechanisms for their effects on DNA methylation.

### **Shared and unique DNA methylation changes**

To elucidate the shared and unique effects of microbiota, *IL10* deficiency, and AOM treatment on DNA methylation, a multi-variate linear regression model that incorporates data from all 42 mice studied was built. Using a False Discovery Rate (FDR) of 0.05, we found that the linear model recapitulated the trends seen in the individual comparisons. Using this model (**Figure 3a**), we determined that microbiota (SPF) induced changes in 13.5% of CpG sites (6.9% hyper and 6.5% hypomethylated), IL10KO induced changes in 10.5% of sites (9% hyper and 1.5% hypomethylated), while AOM induced changes in 5.9% of sites (1% hyper and 4.9% hypomethylated). AOM continued to show a pronounced hypomethylating effect, while IL10KO continued to show a strong hypermethylating effect. Microbiota show roughly equal hypomethylating and hypermethylating effects. We used UpSet plots to determine the overlap in effects of the different factors on CpG methylation, examined separately for hypomethylation (**Figure 3b**) and hypermethylation (**Figure 3c**). Microbiota and IL10KO have the most shared events, particularly when it came to hypermethylation. Thus, of 865 sites hypermethylated by microbiota, 671 (78%) were also affected by IL10KO. There was less conservation when it came to hypomethylation (22% of sites affected by microbiota were also affected by IL10KO). AOM had mostly unique effects. These data suggest that microbiota and IL10KO have shared mechanisms of affecting DNA methylation, while AOM has an independent mechanism of action.

### **The microbiota and inflammation accelerate age-related methylation drift**

Methylation drift characterized by a global loss of DNA methylation with simultaneous hypermethylation in CGI promoters occurs as a result of ageing [32,33]. To compare this to microbiota effects, we

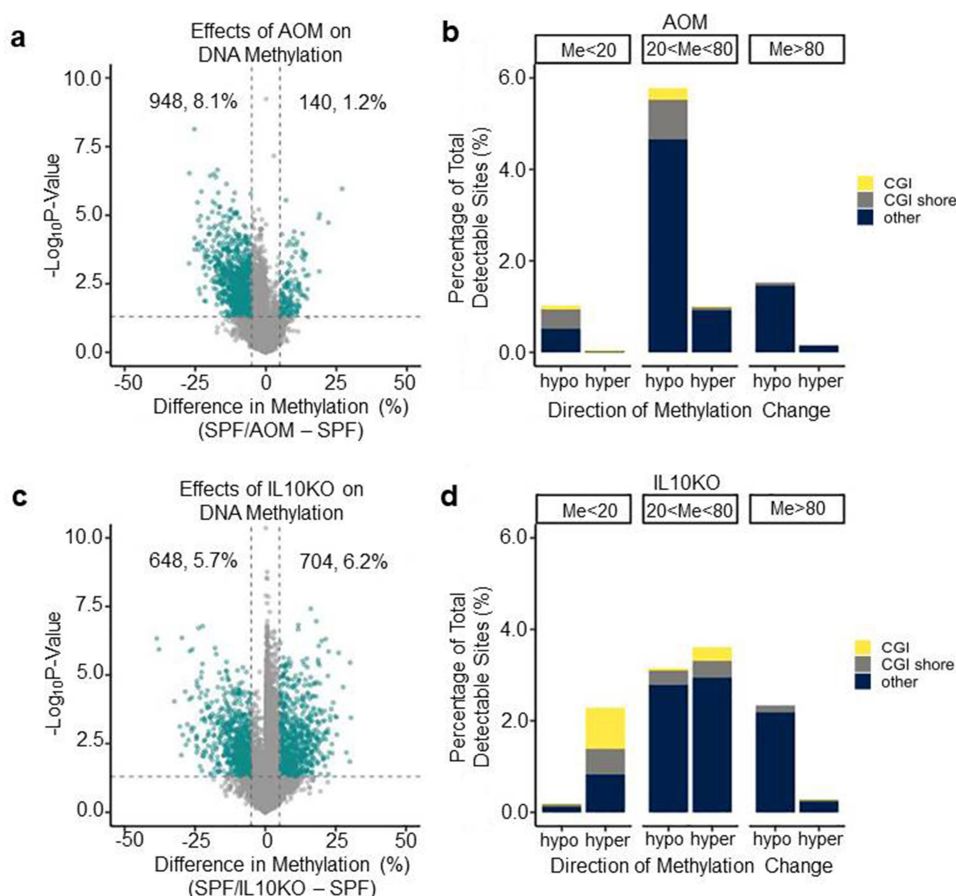


**Figure 2.** AOM is a potent hypomethylating carcinogen. (a) Volcano plot analysis showing methylation differences between SPF and SPF+AOM mice. See Figure 1 for graph details. (b) Bar graph showing the proportion and type of CpG sites that change at least 5% in (a). (c) Volcano plot analysis showing methylation differences between SPF and SPF-*Il10*<sup>-/-</sup> mice. See Figure 1 for graph details. (d) Bar graph showing the proportion and type of CpG sites that change at least 5% in (c).

first generated DREAM data for old (aged 30–33 months) and young (aged 4 months) mouse colon (Figure 4a). A different strain was used for the ageing studies; however, a comparison between ageing and strain differential methylated regions showed little overlap, suggesting that it is exceedingly unlikely that the results presented in the paper can be explained by strain-specific effects (Supplementary Figure S6). Looking at ageing in C57/Bl6 WT mice, we found that of ~20,000 detectable CpG sites, 6.6% decreased in methylation, and 11.5% increased in methylation. Hypermethylated CGIs accounted for 7% of the changes. We analysed the overlap between sites that changed during methylation due to ageing and sites that changed due to microbiota, IL10KO, or AOM. Ageing had the largest effect individually, but there were many shared hypomethylation (Figure 4b) and hypermethylation (Figure 4c) events between ageing and the extrinsic exposures. For

example, out of 472 sites hypomethylated upon microbiota exposure, 139 (29%) were also affected by age; of the 272 hypomethylated sites affected by IL10KO, 31% were also affected by age; of the 1121 sites hypomethylated in inflamed mice (IL10KO/SPF), 31% were hypomethylated as well in ageing mice. Similarly, out of 166 sites hypermethylated upon microbiota exposure, 18% were also affected by age; of the 199 sites affected by IL10KO, 33% were also affected by age; of the 926 sites hypermethylated in inflamed mice (IL10KO/SPF), 35% were also hypermethylated in ageing mice. This corroborates previous data demonstrating partial overlap between inflammation-related and age-related methylation [39], and implicates microbiota in this process.

One drawback of this analysis is the use of a threshold of 5% change in average methylation to consider a site affected by inflammation, microbiota, or ageing; this threshold could lead to

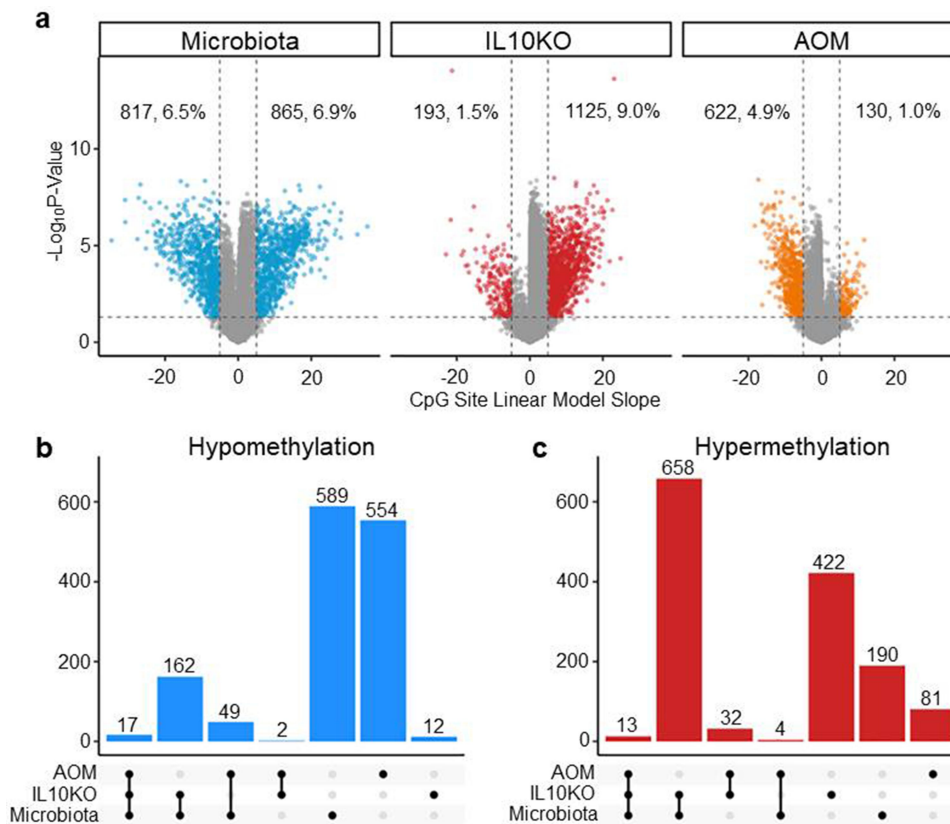


**Figure 3.** Linear regression model of the effects of microbiota, *IL10*<sup>-/-</sup> and AOM on DNA methylation. (a) Shows Volcano plots of FDR (0.05) corrected significant methylation changes attributed to each external exposure. The x-axis indicates the linear model slope for individual CpG sites (equivalent to % change in methylation) while the y-axis is the negative log(10) of the q-value. (b) Shows UpSet plots of shared/unique hypomethylation events while (c) shows UpSet plots of shared/unique hypermethylation events. The number of shared or uniquely altered CpG sites is indicated on top of each vertical bar.

underestimation of conservation because of sites that may change at a lower magnitude in one condition. To address this, we focused on the large number of sites that change with age and generated scatter plots comparing a site's average change with age to change caused by exposures (Figure 4d). Interestingly, the correlation coefficients were positive and statistically significant for all exposures with the strongest correlations for inflammation (IL10KO/SPF,  $r = 0.46$ ,  $p < 0.0001$ ) followed by microbiota ( $r = 0.39$ ,  $p < 0.0001$ ), AOM exposure ( $r = 0.36$ ,  $p < 0.0001$ ), and IL10 deficiency ( $r = 0.09$ ,  $p < 0.0001$ ). Taken together, these data indicate that the vast majority of sites that change with ageing were affected by microbiota or inflammation (combination of microbiota and IL10KO). There were also sites affected by exposures but not by ageing (Supplementary Figure S2), most

evident in mice with inflammation triggered by the combined effects of microbiota and IL10KO.

To get a sense of the functional impact of the genes which have concordant DNA methylation changes between ageing and microbiota in the logistic regression model, we performed pathway analysis on promoters containing at least one CpG site concordant between ageing and microbiota. We found that these promoters are enriched in 42 statistically significant pathways ( $p < 0.05$ , corrected by FDR), including 11 pathways with more than 10 promoters (Supplementary Figure S5). Interestingly, these include 4 that are related to the G-protein-coupled receptor (GPCR) pathway (GPCR ligand binding, G alpha (i) signalling events, signalling by GPCR, and GPCR downstream signalling). Overall, notable enriched pathways suggest potential effects on cell membrane proteins that respond to external signals and help

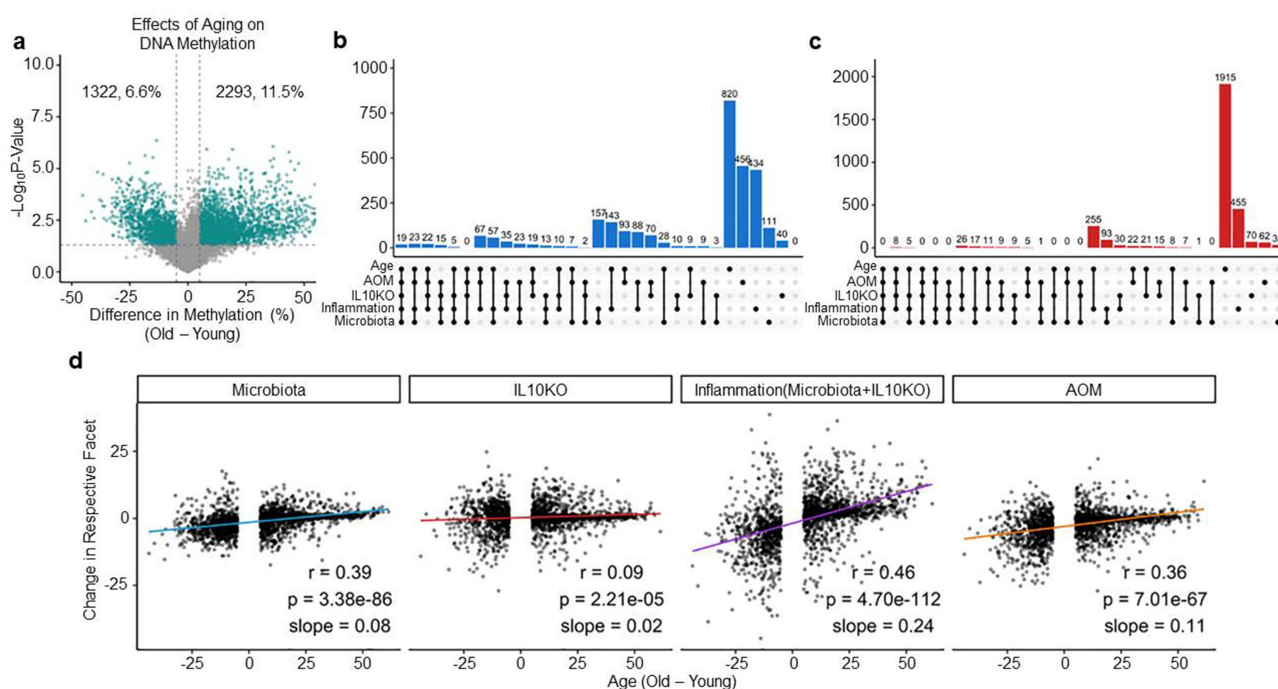


**Figure 4.** Microbiota and inflammation modify the same CpG sites subject to age-related methylation drift. (a) Volcano plot analysis showing methylation differences between young and old mice. See Figure 1a for graph details. (b) UpSet plots of shared/unique hypomethylation events between sites that decrease at least 5% during ageing and in the different exposures analysed in Figures 1–3. ‘Inflammation’ refers to *Il10*<sup>−/−</sup>/SPF mice. (c) Same analysis as in B for sites that increase methylation at least 5%. (d) Scatter plot of average methylation change with age (x-axis) to average change by exposures (y-axis) for all sites that change at least 5% with age. Pearson  $r$ ,  $p$ -value, and slope are indicated in each plot.

regulate transcription, as well as proteins involved in cell–cell communication.

### Bisulphite and gene expression based validation

DREAM is based on differential restriction enzyme analysis and previously validated when compared to bisulphite-based data. To confirm this in the current data set, we randomly selected an affected promoter CpG island, *Trhde*, and studied it by bisulphite-pyrosequencing. As shown in Supplementary Figure S4, methylation of *Trhde* was lowest in WT-GF mice, and was increased by exposure to SPF, by *Il10*-KO, by the combination of the two, but not by AOM treatment. These data closely mirrored what we observed by DREAM analysis. We next examined *Trhde* gene expression by qRT-PCR. We had limited tissues available for gene expression analysis but were able to demonstrate that *Trhde* is repressed in the presence of microbiota (Supplementary Figure S3), consistent with the finding of increased promoter CpG island

methylation. As a control, we examined *Srrm4*, a gene unaffected by DNA methylation, and found no difference in gene expression (Supplementary Figure S3).

### CpG sites affected by microbiota are hypermethylated in colon cancer

To determine the impact of microbiota, inflammation, and/or ageing on methylation in colon cancer, we analysed data from The Cancer Genome Atlas (TCGA). To correspond mouse to human data, we focused on promoters (defined as −1500 to 500 of transcription start site) and used data on the CpG site closest to the transcription start site. Converging DREAM data with TCGA data, we were able to analyse 2,042 genes in total. Figure 5a shows scatter plots of methylation changes in colon cancer patients included in the TCGA data set ( $\beta$  value of methylation difference between tumour and normal) plotted on the y-axis, and methylation changes in our datasets (based on the volcano plot for ageing and on the linear model for individual factors) plotted on the

x-axis. The plots demonstrate a strong concordance between methylation changes in TCGA and each of ageing, microbiota exposure, and *IL10* deficiency. We calculated odds ratios to quantitate this concordance, at a threshold of 5% change in TCGA and in the risk factors (Figure 5b). For hypermethylation, the odds ratios for enrichment were 15.5 (95% CI: [10.6,22.9];  $q = 3.0 \times 10^{-54}$ ) for age, 0 (95% CI: [0,0];  $q = 1$ ) for azoxymethane, 2.3 (95% CI: [1.1,4.5];  $q = 0.039$ ) for *IL10*KO, and 4.1 (95% CI: [1.8,9.0];  $q = 9.4 \times 10^{-4}$ ) for microbiota. For hypomethylation, odds ratios were 2.0 (95% CI: [0.04,13.9];  $q = 0.47$ ) for age, 9.4 (95% CI: [1.6,38.9];  $q = 0.015$ ) for azoxymethane, 9.2 (95% CI: [0.2,116.2];  $q = 0.18$ ) for *IL10*KO and 11.5 (95% CI: [2.6,41.1];  $q = 0.003$ ) for microbiota. Thus, as previously reported, ageing has a major impact on whether a gene becomes hypermethylated in cancer, but we also find that genes affected by microbiota and by *IL10* deficiency are also overrepresented among genes hypermethylated in CRC.

## Discussion

We show here that the presence of a microbiota is associated with changes in DNA methylation that affect 5% of the detectable CpG sites, a high number when one considers the fact that DNA methylation is very carefully controlled with relatively low levels of inter-individual variability [3]. These

effects are compounded by the presence of inflammation – mice with both *IL10* deficiency and exposure to a microbiota showed alterations in 18% of the detectable CpG sites, and the differences were particularly striking at CpG islands, regions that are normally very stable and highly protected from DNA methylation [40]. This strikingly high number is quantitatively similar to what can be seen when comparing mice at the extremes of their lifespan [34], and the pattern of change is very similar to what can be seen in colon cancers (CGI hypermethylation, intergenic hypomethylation). Indeed, CpG sites affected by microbiota are overrepresented among genes hypermethylated in colon cancer, suggesting that microbiota could have an important influence on shaping cancer epigenomes, as previously suggested [28]. Interestingly, while the presence of microbiota accelerates age-related methylation drift, there are also epigenetic changes specific to the different extrinsic factors studied (microbiota, inflammation, AOM) suggesting distinct mechanisms rather than non-specific effects of cycles of injury and stem cell proliferation. It is also worth noting that the effects we observe are related to pathogen-free microbiota. It would be interesting to determine whether more profound changes are seen when pathogenic bacteria are introduced into the mix.

Our results are consistent with recent studies but extend the findings substantially. Three studies

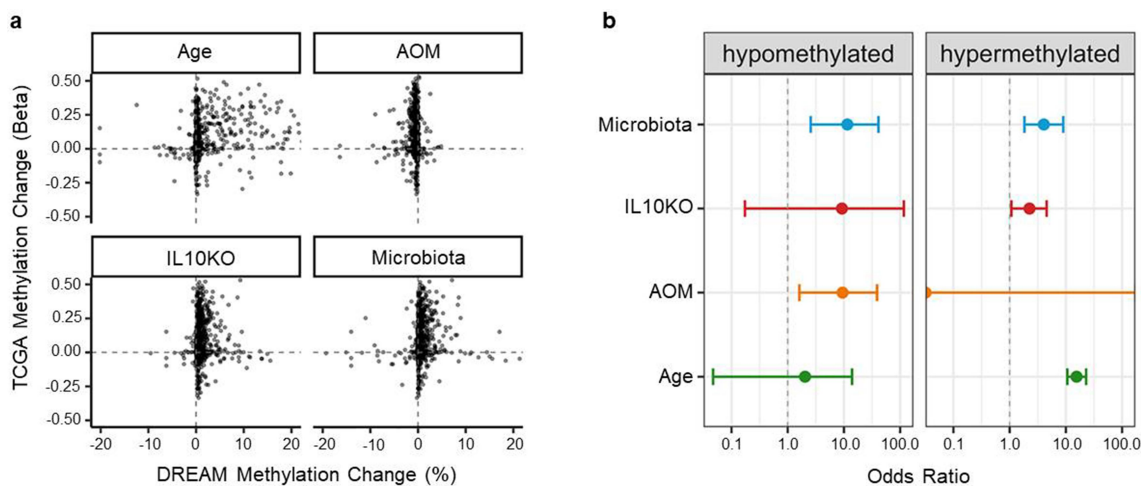


**Figure 5.** Genes affected by extrinsic exposures are more likely to be altered in cancer. (a) Scatter plot of DNA methylation change by ageing or exposure (x-axis) compared to DNA methylation change in colon cancer TCGA samples. (b) Odds ratios compute enrichment of genes altered by ageing or different extrinsic exposures among genes altered in colon cancer (TCGA data). The odds ratios are computed separately for gene promoters hypomethylated (left) or hypermethylated (right) by exposures and in colon cancer.

reported that microbiota affect the physiology and DNA methylation patterns in developing intestinal epithelium [41–43]. Interestingly, the effects seen were primarily outside promoters (e.g., 3' end of genes and inter-genic areas), while our results highlight the profound effect of microbiota and inflammation on promoter CpG islands – the compartment most uniquely affected in ageing and cancer [1]. Ansari also studied the effects of inflammation induced by Dextran Sodium Sulphate on DNA methylation, and found primarily hypomethylation [43], in marked contrast to what we observed with inflammation induced by the combination of IL10 deficiency and the presence of microbiota. Dextran Sodium Sulphate's effects are reminiscent of what we observed with exposure to azoxymethane and raise the possibility that the effects seen are related to the chemical's effect more directly than to inflammation. The effect of DNA damage by azoxymethane on DNA methylation is an important possibility. Increased  $\gamma$ H2AX<sup>+</sup> nuclear foci were observed in AOM/*Il10*<sup>-/-</sup> mice with *E. coli* NC101 in colon [23]; however, we do not know if DNA damage induced by AOM per se is contributing to the altered methylation patterns we are observing. Finally, Sobhani et al. introduced into germ-free mice human faecal microbiota from patients with colon cancer or controls and also observed alterations in DNA methylation [44], and some of the genes affected (such as *SFRP1*) are known to show age-related methylation in the human colon [45]. In our study, we show that even pathogen-free microbiota affect DNA methylation at relatively high levels. Our data uniquely highlight the effects of microbiota and inflammation on aberrant CpG island DNA methylation and link it to the acceleration of ageing effects on DNA methylation. The data also suggest that microbiota/inflammation effects are potential precursors to the aberrant DNA methylation seen in colorectal cancers.

The mechanism by which microbiota affect DNA methylation remains to be elucidated. One possibility is via the production of metabolites which act as cofactors or inhibitors for epigenetic enzymes. For example, the microbial metabolites acetate, propionate, and butyrate are capable of inducing mass reprogramming of histone methylation and acetylation states [24]. Bacterial species producing these short-chain fatty acid metabolites

are known to be decreased in cancer and inflammation. DNA methyltransferases (DNMTs) have been shown to interact with modifications on histone tails [46], and as histone states change, DNA methylation patterns may as well. Additionally, the gut bacteria may cause alterations in host gene expression that affect the ability of host cells to uptake certain metabolites; for example, it has been demonstrated that *E. coli* is capable of down-regulating a protein responsible for butyrate uptake [47]. Aberrant DNA methylation may also be directly initiated by the overproduction of oncogenic metabolites (oncometabolites). Loss-of-function mutations in citric acid cycle enzymes fumarate hydratase (FH) and succinate dehydrogenase (SDH) result in the accumulation of fumarate and succinate, respectively, [48]. A neomorphic mutation in isocitrate dehydrogenase (IDH) causes the enzyme to produce 2-hydroxyglutarate (2HG) instead of  $\alpha$ -ketoglutarate [49]. Each of these mutations is found in certain types of CIMP positive cancer [50], though they are very rarely observed in colorectal cancer [51]. 2HG binds to and inhibits  $\alpha$ -ketoglutarate dependent TET and methyltransferase enzymes, causing DNA hypermethylation and tumorigenesis [50]. Succinate and fumarate have been shown to inhibit these enzymes *in vitro* and there is overlap between the methylated genes associated with each metabolite anomaly, implying that all three may act via this same mechanism [48]. Thus, it is plausible that bacteria cause aberrant methylation in part via over-production of metabolites that modulate the function of the TET DNA demethylases.

Diet is important to note for its effect on the methylation drift in colorectal cancer and ageing [13,32] and closely associated with the composition of the gut microbiota and the production of the bacterial metabolites mentioned above [52]. Introducing diet as another variable in the study design would be an interesting subject to explore in the future studies.

Previous studies have also shown that inflammation alters the DNA methylome [1,53], though the precise mechanisms by which this occurs are unknown. It has been proposed that inflammation increases cell turnover rate, and inflammation-induced methylation may simply be a reflection

of an increased rate of age-related methylation [13]. The overlap we observed between inflammation and ageing-associated changes is consistent with this. However, we found that microbiota and inflammation also induced methylation changes that were not observed in ageing. It has been suggested that direct interactions with inflammatory cytokines alter a cell's methylation profile [54]. It is also possible that the inflamed gut exerts different selective pressures on the host intestinal epithelial cells than the non-inflamed gut, selecting for cells with unique DNA methylation profiles. It may eventually be possible to tease out inflammation-independent effects of extrinsic factors on DNA methylation.

In conclusion, we find that microbiota have a profound effect on DNA methylation in the gut and help shape the aberrant methylomes seen in ageing and cancer. The fact that extrinsic factors (bacteria, inflammation, carcinogens) modulate the epigenome suggests potential ways to intervene therapeutically for cancer prevention.

### Disclosure statement

No potential conflict of interest was reported by the author(s).

### Data Availability Statement

The datasets supporting the conclusions of this article are available in the GEO (accession number: GSE150333, <https://www.ncbi.nlm.nih.gov/geo/query/acc.cgi?acc=GSE150333>).

A secure token (kjjzmsauldorlc) has been created to allow editors and reviewers to review record GSE150333 while it remains in private status. Further information and requests for resources and reagents should be directed to and will be fulfilled by the Lead Contact, Jean-Pierre J. Issa.

### Author Contributions

AS, CJ, and JI contributed to study design. AS, LC, and HV generated data, and AS, LC, PP, KK, GC, JM, JJ, CJ, and JP analysed data. SM provided key reagents, and CJ provided key samples. AS, PP, LC, KK, and JP contributed to writing the paper, and PP, SM, JM, JJ, and CJ contributed to editing the paper.

### Funding

This work was supported by the National Institutes of Health under Grant R01-CA214005.

### ORCID

Ang Sun  <http://orcid.org/0000-0002-8644-0407>  
 Pyounghwa Park  <http://orcid.org/0000-0002-5850-6181>  
 Himani Vaidya  <http://orcid.org/0000-0002-2779-3069>  
 Shinji Maegawa  <http://orcid.org/0000-0003-2057-7854>  
 Kelsey Keith  <http://orcid.org/0000-0002-7451-5117>  
 Gennaro Calendo  <http://orcid.org/0000-0002-4510-5530>  
 Jozef Madzo  <http://orcid.org/0000-0001-6607-1213>  
 Jaroslav Jelinek  <http://orcid.org/0000-0002-2533-0220>  
 Christian Jobin  <http://orcid.org/0000-0002-3733-1001>  
 Jean-Pierre J. Issa  <http://orcid.org/0000-0003-2258-5030>

### References

- [1] Issa JP. Aging and epigenetic drift: a vicious cycle. *J Clin Invest.* 2014;124(1):24–29.
- [2] Deaton AM, Bird A. CpG islands and the regulation of transcription. *Genes Dev.* 2011;25(10):1010–1022.
- [3] Jelinek J, Liang S, Lu Y, et al. Conserved DNA methylation patterns in healthy blood cells and extensive changes in leukemia measured by a new quantitative technique. *Epigenetics.* 2012;7(12):1368–1378.
- [4] Yang X, Han H, De Carvalho DD, et al. Gene body methylation can alter gene expression and is a therapeutic target in cancer. *Cancer Cell.* 2014;26(4):577–590.
- [5] Baylin SB, Jones PA. A decade of exploring the cancer epigenome - biological and translational implications. *Nat Rev Cancer.* 2011;11(10):726–734.
- [6] Yu DH, Waterland RA, Zhang P, et al. Targeted p16 (Ink4a) epimutation causes tumorigenesis and reduces survival in mice. *J Clin Invest.* 2014;124(9):3708–3712.
- [7] Estécio MR, Gallegos J, Dekmezian M, et al. SINE retrotransposons cause epigenetic reprogramming of adjacent gene promoters. *Mol Cancer Res.* 2012;10(10):1332–1342.
- [8] Zhang Y, Shu J, Si J, et al. Repetitive elements and enforced transcriptional repression co-operate to enhance DNA methylation spreading into a promoter CpG-island. *Nucleic Acids Res.* 2012;40(15):7257–7268.
- [9] Estécio MR, Issa JP. Dissecting DNA hypermethylation in cancer. *FEBS Lett.* 2011;585(13):2078–2086.
- [10] Estécio MR, Gallegos J, Vallot C, et al. Genome architecture marked by retrotransposons modulates predisposition to DNA methylation in cancer. *Genome Res.* 2010;20(10):1369–1382.
- [11] Issa JP, Ahuja N, Toyota M, et al. Accelerated age-related CpG island methylation in ulcerative colitis. *Cancer Res.* 2001;61(9):3573–3577.
- [12] Wallace K, Grau MV, Levine AJ, et al. Association between folate levels and CpG Island hypermethylation in normal colorectal mucosa. *Cancer Prev Res (Phila).* 2010;3(12):1552–1564.
- [13] Sapienza C, Issa JPD. Nutrition, and Cancer Epigenetics. *Annu Rev Nutr.* 2016;36:665–681.

- [14] Chiba T, Marusawa H, Ushijima T. Inflammation-associated cancer development in digestive organs: mechanisms and roles for genetic and epigenetic modulation. *Gastroenterology*. 2012;143(3):550–563.
- [15] Sender R, Fuchs S, Milo R. Revised estimates for the number of human and bacteria cells in the body. *PLoS Biol*. 2016;14(8):e1002533.
- [16] Turnbaugh PJ, Gordon JI. The core gut microbiome, energy balance and obesity. *J Physiol*. 2009;587(Pt 17):4153–4158.
- [17] Sonnenburg JL, Bäckhed F. Diet-microbiota interactions as moderators of human metabolism. *Nature*. 2016;535(7610):56–64.
- [18] Hooper LV, Littman DR, Macpherson AJ. Interactions between the microbiota and the immune system. *Science*. 2012;336(6086):1268–1273.
- [19] Holmes E, Li JV, Marchesi JR, et al. Gut microbiota composition and activity in relation to host metabolic phenotype and disease risk. *Cell Metab*. 2012;16(5):559–564.
- [20] Koppel N, Maini Rekdal V, Balskus EP. Chemical transformation of xenobiotics by the human gut microbiota. *Science*. 2017;356(6344):eaag2770.
- [21] Tazume S, Umehara K, Matsuzawa H, et al. Effects of germfree status and food restriction on longevity and growth of mice. *Jikken Dobutsu*. 1991;40(4):517–522.
- [22] Tsilimigras MC, Fodor A, Jobin C. Carcinogenesis and therapeutics: the microbiota perspective. *Nat Microbiol*. 2017;2:17008.
- [23] Arthur JC, Perez-Chanona E, Mühlbauer M, et al. Intestinal inflammation targets cancer-inducing activity of the microbiota. *Science*. 2012;338(6103):120–123.
- [24] Krautkramer KA, Kreznar JH, Romano KA, et al. Diet-microbiota interactions mediate global epigenetic programming in multiple host tissues. *Mol Cell*. 2016;64(5):982–992.
- [25] Kumar H, Lund R, Laiho A, et al. Gut microbiota as an epigenetic regulator: pilot study based on whole-genome methylation analysis. *MBio*. 2014;5(6):e02113–14.
- [26] Maekita T, Nakazawa K, Mihara M, et al. High levels of aberrant DNA methylation in *Helicobacter pylori*-infected gastric mucosae and its possible association with gastric cancer risk. *Clin Cancer Res*. 2006;12(3 Pt 1):989–995.
- [27] Chang MS, Uozaki H, Chong JM, et al. CpG island methylation status in gastric carcinoma with and without infection of Epstein-Barr virus. *Clin Cancer Res*. 2006;12(10):2995–3002.
- [28] Tahara T, Yamamoto E, Suzuki H, et al. Fusobacterium in colonic flora and molecular features of colorectal carcinoma. *Cancer Res*. 2014;74(5):1311–1318.
- [29] Sellon RK, Tonkonogy S, Schultz M, et al. Resident enteric bacteria are necessary for development of spontaneous colitis and immune system activation in interleukin-10-deficient mice. *Infect Immun*. 1998;66(11):5224–5231.
- [30] Jelinek J, Lee JT, Cesaroni M, et al. Digital restriction enzyme analysis of methylation (DREAM). In: Tost J, editor. *DNA methylation protocols*. New York: Springer New York; 2018. p. 247–265.
- [31] Jelinek J, Madzo J. DREAM: a simple method for DNA methylation profiling by high-throughput sequencing. In: Li S, Zhang H, editors. *Chronic myeloid leukemia: methods and protocols*. methods in molecular biology. 2016;14652016: 111–127.
- [32] Maegawa S, Lu Y, Tahara T, et al. Caloric restriction delays age-related methylation drift. *Nat Commun*. 2017;8(1):539.
- [33] Maegawa S, Gough SM, Watanabe-Okochi N, et al. Age-related epigenetic drift in the pathogenesis of MDS and AML. *Genome Res*. 2014;24(4):580–591.
- [34] Maegawa S, Hinkal G, Kim HS, et al. Widespread and tissue specific age-related DNA methylation changes in mice. *Genome Res*. 2010;20(3):332–340.
- [35] Yu GC, He QY. ReactomePA: an R/Bioconductor package for reactome pathway analysis and visualization. *Mol Biosyst*. 2016;12(2):477–479.
- [36] R Core Team. R: a language and environment for statistical computing. Vienna Austria: R Foundation for Statistical Computing; 2019. <https://www.R-project.org>;
- [37] Ahlmann-Eltze CG. Combination Matrix Axis for 'ggplot2' to Create 'UpSet' Plots. R package version 0.3.0. 2020.
- [38] Uronis JM, Mühlbauer M, Herfarth HH, et al. Modulation of the intestinal microbiota alters colitis-associated colorectal cancer susceptibility. *PLoS One*. 2009;4(6):e6026.
- [39] Hahn MA, Hahn T, Lee DH, et al. Methylation of polycomb target genes in intestinal cancer is mediated by inflammation. *Cancer Res*. 2008;68(24):10280–10289.
- [40] Bird A. DNA methylation patterns and epigenetic memory. *Genes Dev*. 2002;16(1):6–21.
- [41] Yu DH, Gadkari M, Zhou Q, et al. Postnatal epigenetic regulation of intestinal stem cells requires DNA methylation and is guided by the microbiome. *Genome Biol*. 2015;16:211.
- [42] Pan WH, Sommer F, Falk-Paulsen M, et al. Exposure to the gut microbiota drives distinct methylome and transcriptome changes in intestinal epithelial cells during postnatal development. *Genome Med*. 2018;10(1):27.
- [43] Ansari I, Raddatz G, Gutekunst J, et al. The microbiota programs DNA methylation to control intestinal homeostasis and inflammation. *Nat Microbiol*. 2020;5(4):610–619.
- [44] Sobhani I, Bergsten E, Couffin S, et al. Colorectal cancer-associated microbiota contributes to oncogenic epigenetic signatures. *Proc Natl Acad Sci U S A*. 2019;116(48):24285–24295.
- [45] Shen L, Toyota M, Kondo Y, et al. Integrated genetic and epigenetic analysis identifies three different subclasses of colon cancer. *Proc Natl Acad Sci U S A*. 2007;104(47):18654–18659.

- [46] Baubec T, Schübeler D. Genomic patterns and context specific interpretation of DNA methylation. *Curr Opin Genet Dev.* 2014;25:85–92.
- [47] Kumar A, Alrefai WA, Borthakur A, et al. *Lactobacillus acidophilus* counteracts enteropathogenic *E. coli*-induced inhibition of butyrate uptake in intestinal epithelial cells. *Am J Physiol Gastrointest Liver Physiol.* 2015;309(7):G602–7.
- [48] Yang M, Soga T, Pollard PJ. Oncometabolites: linking altered metabolism with cancer. *J Clin Invest.* 2013;123(9):3652–3658.
- [49] Ward PS, Patel J, Wise DR, et al. The common feature of leukemia-associated IDH1 and IDH2 mutations is a neomorphic enzyme activity converting alpha-ketoglutarate to 2-hydroxyglutarate. *Cancer Cell.* 2010;17(3):225–234.
- [50] Figueroa ME, Abdel-Wahab O, Lu C, et al. Leukemic IDH1 and IDH2 mutations result in a hypermethylation phenotype, disrupt TET2 function, and impair hematopoietic differentiation. *Cancer Cell.* 2010;18(6):553–567.
- [51] Tahara T, Yamamoto E, Madireddi P, et al. Colorectal carcinomas with CpG island methylator phenotype 1 frequently contain mutations in chromatin regulators. *Gastroenterology.* 2014;146(2):530–38.e5.
- [52] Leeming ER, Johnson AJ, Spector TD, et al. Effect of diet on the Gut Microbiota: rethinking intervention duration. *Nutrients.* 2019;11(12).
- [53] Niwa T, Tsukamoto T, Toyoda T, et al. Inflammatory processes triggered by *Helicobacter pylori* infection cause aberrant DNA methylation in gastric epithelial cells. *Cancer Res.* 2010;70(4):1430–1440.
- [54] Gasche JA, Hoffmann J, Boland CR, et al. Interleukin-6 promotes tumorigenesis by altering DNA methylation in oral cancer cells. *Int J Cancer.* 2011;129(5):1053–1063.